B anomalies in the nonminimal universal extra dimension model

Jong-Phil Lee*

Sang-Huh College, Konkuk University, Seoul 05029, Korea

(Received 19 June 2019; published 2 October 2019)

We investigate B anomalies in the framework of the nonminimal universal extra dimension model. Newly measured polarization parameters in $B \to D^{(*)}\tau\nu$, $P_\tau(D^{(*)})$, and $F_L(D^*)$ as well as the ratios $R(D^{(*)})$ are considered altogether. The Kaluza-Klein modes of the W boson and charged scalar contributes to the new physics effects. We find that the model parameters fit the global data very well with the minimum χ^2/d.o.f. near unity, rendering $B_c \to \tau\nu$ branching ratios to be a few percent. The best-fit values of $R(D)$ and $R(D^*)$ are still far from ($\gtrsim 2\sigma$) the standard model predictions.

DOI: 10.1103/PhysRevD.100.075005

I. INTRODUCTION

The standard model (SM) of particle physics has been up to now very successful in explaining many phenomena in our Universe. The last missing piece of the SM, the Higgs particle, was finally discovered in 2012. But there must be some new physics (NP) beyond the SM. Flavor physics is a good testing ground for the NP. Recently, some anomalies were reported in $b \to c$ semileptonic decays. The fraction of the branching ratios

$$R(D^{(*)}) \equiv \frac{\mathrm{Br}(B \to D^{(*)}\tau\nu)}{\mathrm{Br}(B \to D^{(*)}\ell\nu)} \tag{1}$$

reveals an excess over the SM predictions [1],

$$\begin{aligned} R(D)_{\mathrm{SM}} &= 0.299 \pm 0.003, \\ R(D^*)_{\mathrm{SM}} &= 0.258 \pm 0.005. \end{aligned} \tag{2}$$

Experiments including *BABAR*, Belle, and LHCb have reported somewhat larger values of $R(D^{(*)})$ than those of Eq. (2) by about $2\sigma \sim 3\sigma$ [2–11]. Recently, the Belle Collaboration announced new results [9],

$$\begin{aligned} R(D)_{\mathrm{Belle1904}} &= 0.307 \pm 0.037 \pm 0.016, \\ R(D^*)_{\mathrm{Belle1904}} &= 0.283 \pm 0.018 \pm 0.014, \end{aligned} \tag{3}$$

which are closer to Eq. (2) than the previous data and consistent with the SM within 1.2σ. Combined results for all data by the Heavy Flavor Averaging Group (HFLAV) Collaboration [12],

$$\begin{aligned} R(D)_{\mathrm{HFLAV}} &= 0.340 \pm 0.027 \pm 0.013, \\ R(D^*)_{\mathrm{HFLAV}} &= 0.295 \pm 0.011 \pm 0.008, \end{aligned} \tag{4}$$

give a discrepancy between the SM predictions and experimental data at the 3.08σ level. The *BABAR* measurements [2,3] exclude at the 99.8% confidence level the type-II two-Higgs-doublet model (2HDM) where a charged Higgs boson contributes to $R(D^{(*)})$, while the Belle measurements [4] are compatible with the type-II 2HDM. It was shown that an anomalous τ coupling to the charged Higgs in the 2HDM can explain the data very well [13]. In extra dimension models the overlapping between the wave functions of τ and the neutral scalar could be weak to make τ screened from the scalar vacuum, resulting in an enhancement of τ couplings to charged Higgs. For discussions in the 2HDM, see Refs. [14–19]. There are many other NP scenarios to explain the $R(D^{(*)})$ anomaly, including leptoquark models [20–26], composite models [27–30], warped extra dimensions [31–34], etc. [35–37].

On top of the ratio $R(D^{(*)})$ the Belle Collaboration measured the relevant polarizations in $B \to D^{(*)}\tau\nu$ decays. One can consider observable parameters associated with D^* as well as τ. The τ-polarization asymmetry is defined as

$$P_\tau(D^{(*)}) \equiv \frac{\Gamma_\tau^{D^{(*)}}(+) - \Gamma_\tau^{D^{(*)}}(-)}{\Gamma_\tau^{D^{(*)}}(+) + \Gamma_\tau^{D^{(*)}}(-)}, \tag{5}$$

where $\Gamma_\tau^{D^{(*)}}(\pm)$ is the decay width for $(\pm)\tau$ helicity. The SM predictions are [38,39]

*jongphil7@gmail.com

$$P_\tau(D)_{\rm SM} = 0.325 \pm 0.009,$$
$$P_\tau(D^*)_{\rm SM} = -0.497 \pm 0.013. \quad (6)$$

The experimental result is [7,8]

$$P_\tau(D^*) = -0.38 \pm 0.51^{+0.21}_{-0.16}. \quad (7)$$

The longitudinal D^* polarization is

$$F_L(D^*) \equiv \frac{\Gamma(B \to D_L^* \tau\nu)}{\Gamma(B \to D^* \tau\nu)}, \quad (8)$$

where the Belle's measurement is [40]

$$F_L(D^*) = 0.60 \pm 0.08 \pm 0.035, \quad (9)$$

while the SM value is estimated to be [41]

$$F_L(D^*)_{\rm SM} = 0.46 \pm 0.04. \quad (10)$$

The polarization parameters could provide more information about the Lorentz structure of possible NP.

In this paper we consider the nonminimal universal extra dimension (NMUED) model [42–49] to fit the global data on $R(D^{(*)})$ and polarization parameters. In the universal extra dimension (UED) models there is an extra spacelike dimension with a flat metric compactified on an S^1/Z_2 orbifold, where the SM particles could reside. Each SM particles is accompanied by infinite towers of Kaluza-Klein (KK) states. There are two branes at the end points of the orbifold. The reflection symmetry of the bulk space provides with the KK-parity conservation. The lightest KK particle is a natural candidate for dark matter, which makes the UED scenario a strong alternative to the SM. As discussed in Ref. [50], in the minimal version of the UED (MUED) there are no new couplings at the tree level relevant to $R(D^{(*)})$. The radiative corrections include bulk corrections and boundary localized ones. In the MUED models the latter is adjusted to cancel the cutoff dependent corrections. The NMUED models allow the boundary localized terms (BLTs) to be free parameters. In this analysis we include the BLTs with free strength parameters. The presence of BLTs changes mass spectrum and couplings of KK modes of the UED model. The NP effects enter through the possible interactions between a pair of zero-mode fermion and even KK modes of charged gauge boson or scalar associated with the BLTs [50,51]. These kinds of interactions are not allowed in the MUED because of the KK wave function orthogonality. Since the new interactions contribute to $R(D^{(*)})$ at tree level, we expect the NMUED model would provide some hints to solve the $R(D^{(*)})$ puzzle.

The paper is organized as follows. In Sec. II the NMUED model is introduced. Section III provides the various observables in numerical forms. The results and discussions are given in Sec. IV, and we conclude in Sec. V.

II. NMUED MODEL

We assume that there is one flat extra dimension (y) compactified on an S^1/Z_2 orbifold with radius R. Two branes are located at the end points $y = 0$ and $y = \pi R$ where both boundary terms are equal. The five-dimensional (5D) action for fermions f is [50]

$$\begin{aligned}\mathcal{S}_f = \sum_{f=q,\ell} \int d^4x \int_0^{\pi R} dy \{ & i\bar{\Psi}_L^f \Gamma^M \mathcal{D}_M \Psi_L^f \\ & + r_f[\delta(y) + \delta(y-\pi R)] i\bar{\Psi}_L^f \gamma^\mu \mathcal{D}_\mu P_L \Psi_L^f + i\bar{\Psi}_R^f \Gamma^M \mathcal{D}_M \Psi_R^f \\ & + r_f[\delta(y) + \delta(y-\pi R)] i\bar{\Psi}_R \gamma^\mu \mathcal{D}_\mu P_R \Psi_R^f \}, \end{aligned} \quad (11)$$

where $\Psi_{L,R}^f(x,y)$ are the 5D four component Dirac spinors for fermions $f = q, \ell$. In terms of two component spinors,

$$\Psi_{L,R}^f(x,y) = \begin{pmatrix} \psi_{L,R}^f(x,y) \\ \chi_{L,R}^f(x,y) \end{pmatrix} = \sum_n \begin{pmatrix} \psi_{L,R}^{f(n)}(x) F_{L,R}^{f(n)}(y) \\ \chi_{L,R}^{f(n)}(x) G_{L,R}^{f(n)}(y) \end{pmatrix}, \quad (12)$$

where $F_{L,R}^{f(n)}(y)$ and $G_{L,R}^{f(n)}(y)$ are the nth KK wave functions. In Eq. (11) r_f is the strength of the boundary localized terms. They are related to the mass of the nth KK excitation $m_{f^{(n)}}$ by the transcendental equation

$$\frac{r_f m_{f^{(n)}}}{2} = \begin{cases} -\tan\left(\frac{m_{f^{(n)}}\pi R}{2}\right) & \text{for even } n, \\ \cot\left(\frac{m_{f^{(n)}}\pi R}{2}\right) & \text{for odd } n. \end{cases} \quad (13)$$

As for the gauge boson sector, the 5D action is

$$\begin{aligned}\mathcal{S}_{\rm gauge} = -\frac{1}{4} \int d^4x \int_0^{\pi R} dy \{ & W_{MN}^i W^{iMN} \\ & + r_V[\delta(y) + \delta(y-\pi R)] W_{\mu\nu}^i W^{i\mu\nu} \\ & + B_{MN} B^{MN} + r_V[\delta(y) + \delta(y-\pi R)] B_{\mu\nu} B^{\mu\nu} \}, \end{aligned} \quad (14)$$

where W_{MN}^i, B_{MN} are the 5D gauge field strength tensors. The nth KK mass of the gauge boson is

$$M_{W^{(n)}} = \sqrt{M_W^2 + m_{V^{(n)}}^2}, \quad (15)$$

where $m_{V^{(n)}}$ satisfies the same transcendental equation as Eq. (13). For the 5D scalar field $\Phi(x,y)$, the action is

$$\mathcal{S}_\phi = \int d^4x \int_0^{\pi R} dy\{(\mathcal{D}_M\Phi)^\dagger(\mathcal{D}^M\Phi) + r_\phi[\delta(y)+\delta(y-\pi R)](\mathcal{D}_\mu\Phi)^\dagger(\mathcal{D}^\mu\Phi)\}. \quad (16)$$

We choose $r_\phi = r_V$ for proper gauge fixing [52], and consequently the mass of the KK scalar is $m_{\phi^{(n)}} = m_{V^{(n)}}$. The Yukawa interaction is described by

$$\mathcal{S}_Y = -\sum_f \int d^4x \int_0^{\pi R} dy\{\lambda_5\bar{\Psi}_L^f\tilde{\Phi}\Psi_R^f + r_Y[\delta(y)+\delta(y-\pi R)]\lambda_5\bar{\psi}^f{}_L\tilde{\Phi}\chi_R^f + \text{H.c.}\}, \quad (17)$$

where λ_5 is the 5D Yukawa coupling and r_Y is the boundary strength.

In NMUED new KK particles contribute to B decays. As mentioned in Sec. I, even KK modes of the W boson as well as the charged Higgs couple to a pair of zero-mode fermions, which provide new vector and scalar interactions, respectively. The effects are encoded in the overlap integrals

$$I_n^{fg} = \sqrt{\pi R\left(1+\frac{r_V}{\pi R}\right)} \times \int_0^{\pi R} dy\{1+r_f[\delta(y)+\delta(y-\pi R)]\}a^n F_L^{f(0)}F_L^{f(0)},$$
$$I_n^{fY} = \sqrt{\pi R\left(1+\frac{r_V}{\pi R}\right)} \times \int_0^{\pi R} dy\{1+r_Y[\delta(y)+\delta(y-\pi R)]\}f^n F_L^{f(0)}G_R^{f(0)}, \quad (18)$$

where a^n and h^n are nth KK mode of the W boson and scalar, respectively. For $r_\phi = r_V$ and $a^n = h^n$, and further if $r_f = r_Y$, then [50]

$$I_n^{fg} = I_n^{fY} \equiv I_n^f = \frac{\sqrt{2}(\hat{r}_f-\hat{r}_V)\sqrt{1+\hat{r}_V}}{(1+\hat{r}_f)\sqrt{1+r_V^2 m_{V^{(n)}}^2/4+\hat{r}_V}}, \quad (19)$$

where $\hat{r} \equiv r/(\pi R)$. Actually, I_n^f is the interaction term between a pair of zero-mode fermion f and nth KK modes of W boson or scalar, which encodes the NP effects on observables.

III. OBSERVABLES

Now the effective Hamiltonian for $b \to c\ell\nu$ is

$$\mathcal{H}_{\text{eff}} = \frac{4G_F}{\sqrt{2}}V_{cb}\sum_{\ell=\mu,\tau}\{(1+C_V^\ell)\mathcal{O}_V^\ell + C_S^\ell\mathcal{O}_S^\ell\}, \quad (20)$$

where the operators $\mathcal{O}_{V,S}^\ell$ are defined by

$$\mathcal{O}_V^\ell = (\bar{c}_L\gamma^\mu b_L)(\bar{\ell}_L\gamma_\mu\nu_{\ell L}), \quad (21)$$

$$\mathcal{O}_S^\ell = (\bar{c}_L b_R)(\bar{\ell}_R\nu_{\ell L}). \quad (22)$$

The NP effects are encapsulated in the Wilson coefficients $C_{V,S}^\ell$ given as [50]

$$C_V^\ell = \sum_{n\geq 2}\left[\frac{M_W^2}{M_{W^{(n)}}^2}\right]I_n^q I_n^\ell, \quad (23)$$

$$C_S^\ell = \sum_{n\geq 2}\left[\frac{m_b m_\ell}{M_{W^{(n)}}^2}\right]\left[\frac{M_W^2}{M_{W^{(n)}}^2}\right]\left\{\cos\left(\frac{1}{2}\tan^{-1}\left[\frac{m_c}{m_{f^{(n)}}}\right] - \frac{1}{2}\tan^{-1}\left[\frac{m_\ell}{m_{f^{(n)}}}\right]\right) - \sin\left(\frac{1}{2}\tan^{-1}\left[\frac{m_c}{m_{f^{(n)}}}\right] + \frac{1}{2}\tan^{-1}\left[\frac{m_\ell}{m_{f^{(n)}}}\right]\right)\right\}I_n^q I_n^\ell. \quad (24)$$

From $\mathcal{H}_{\text{eff}}$ one can calculate the transition amplitudes and decay rates for $B \to D^{(*)}$ decays and can construct various observable parameters. We concentrate only on the numerical results for the observables in our analysis. Numerically the observables for $B \to D^{(*)}\ell\nu_\ell$ decays are (at $\mu = m_b$ scale) [53]

$$R(D) = 2R_{\text{SM}}(D)\frac{(1+C_V^\tau)^2 + 1.54(1+C_V^\tau)C_S^\tau + 1.09(C_S^\tau)^2}{1+(1+C_V^\mu)^2 + 1.54(1+C_V^\mu)C_S^\mu + 1.09(C_S^\mu)^2}, \quad (25)$$

$$R(D^*) = 2R_{\text{SM}}(D^*)\frac{(1+C_V^\tau)^2 + 0.13(1+C_V^\tau)C_S^\tau + 0.05(C_S^\tau)^2}{1+(1+C_V^\mu)^2 + 0.13(1+C_V^\mu)C_S^\mu + 0.05(C_S^\mu)^2}, \quad (26)$$

$$P_\tau(D) = \frac{0.32(1+C_V^\tau)^2 + 1.54(1+C_V^\tau)C_S^\tau + 1.09(C_S^\tau)^2}{(1+C_V^\tau)^2 + 1.54(1+C_V^\tau)C_S^\tau + 1.09(C_S^\tau)^2}, \quad (27)$$

TABLE I. Experimental data for $R(D^{(*)})$, $P_\tau(D^{(*)})$, and $F_L(D^*)$. The uncertainties are $\pm$(statistical) $\pm$ (systematic). For the third uncertainty of LHCb(1711), see Ref. [11] for details. For *BABAR*, Belle(2015), and Belle(2019) results, the correlations between $R(D)$ and $R(D^*)$ are -0.31, -0.50, and -0.51, respectively [12].

	$R(D)$	$R(D^*)$
BABAR	$0.440 \pm 0.058 \pm 0.042$	$0.332 \pm 0.024 \pm 0.018$ [3]
Belle(2015)	$0.375 \pm 0.064 \pm 0.026$	$0.293 \pm 0.038 \pm 0.015$ [4]
Belle(2016)	...	$0.302 \pm 0.030 \pm 0.011$ [5]
Belle(2017)	...	$0.276 \pm 0.034^{+0.029}_{-0.026}$ [6]
Belle(2017)	...	$0.270 \pm 0.035^{+0.028}_{-0.025}$ [7,8]
Belle(2019)	$0.307 \pm 0.037 \pm 0.016$	$0.283 \pm 0.018 \pm 0.014$ [9]
LHCb(2015)	...	$0.336 \pm 0.027 \pm 0.030$ [10]
LHCb(2017)	...	$0.291 \pm 0.019 \pm 0.026 \pm 0.013$ [11]
	$P_\tau(D^*)$	$F_L(D^*)$
Belle(2017)	$-0.38 \pm 0.51^{+0.21}_{-0.16}$ [7,8]	...
Belle(2019)	...	$0.60 \pm 0.08 \pm 0.04$ [40]

$$P_\tau(D^*) = \frac{-0.49(1+C_V^\tau)^2 + 0.13(1+C_V^\tau)C_S^\tau + 0.05(C_S^\tau)^2}{(1+C_V^\tau)^2 + 0.13(1+C_V^\tau)C_S^\tau + 0.05(C_S^\tau)^2}, \tag{28}$$

$$F_L(D^*) = \frac{0.46(1+C_V^\tau)^2 + 0.13(1+C_V^\tau)C_S^\tau + 0.05(C_S^\tau)^2}{(1+C_V^\tau)^2 + 0.13(1+C_V^\tau)C_S^\tau + 0.05(C_S^\tau)^2}, \tag{29}$$

$$\mathrm{Br}(B_c \to \tau\nu) = 0.02\left(\frac{f_{B_c}}{0.43\ \mathrm{GeV}}\right)[1 + C_V^\tau + 4.3C_S^\tau]^2. \tag{30}$$

The results are obtained from the numerical values of the relevant form factors of $B \to D$ [54] and $B \to D^*$ transitions [1,55].

The branching ratio of $B_c \to \tau\nu$, $\mathrm{Br}(B_c \to \tau\nu)$ could impose strong constraints on $R(D^{(*)})$ [56]. Since $\mathrm{Br}(B_c \to \tau\nu) \sim (1 + C_V^\tau + 4.3C_S^\tau)^2$, the branching ratio directly affects the relevant Wilson coefficients. There are still debates on the upper bound of $\mathrm{Br}(B_c \to \tau\nu)$. The strongest bound is from Ref. [57], where $\mathrm{Br}(B_c \to \tau\nu) < 10\%$. On the other hand, Ref. [53] argues that the branching ratio could be as large as 60%. In this analysis we do not explicitly impose the $\mathrm{Br}(B_c \to \tau\nu)$ constraints because, as we will see later, our results are compatible with small values of $\mathrm{Br}(B_c \to \tau\nu)$. The experimental data for various observables used in this analysis are listed in Table I.

IV. RESULTS

We implement the global χ^2 fit for the observables in Table I. We first define χ^2 as

$$\chi^2 \equiv \sum_{i,j} [\mathcal{O}_i^{\mathrm{exp}} - \mathcal{O}_i^{\mathrm{th}}] \mathcal{C}_{ij}^{-1} [\mathcal{O}_j^{\mathrm{exp}} - \mathcal{O}_j^{\mathrm{th}}], \tag{31}$$

where $\mathcal{O}_i^{\mathrm{exp}}$ are the experimental data, while $\mathcal{O}_i^{\mathrm{th}}$ are the theoretical predictions of Eqs. (25)–(30), and $\mathcal{C}_{ij}$ are the correlation matrix elements.

There are two major constraints. One is from the oblique parameters of the electroweak precision test (EWPT) [58–61]. In the NMUED model the Fermi constant is modified by the tree-level contributions of even nth KK modes of W bosons to the four-fermion interactions. This kind of correction is absent in the MUED scenario. The Fermi constant in NMUED is now written as

$$G_F = G_F^0 + \delta G_F. \tag{32}$$

Here G_F^0 is the Fermi constant in the SM and δG_F is the correction from the new contributions of the $W^\pm$ KK modes. Explicitly [50],

$$G_F^0 = \frac{g^2}{4\sqrt{2}M_W^2}, \qquad \delta G_F = \sum_{n\geq 2} \frac{g^2 (I_n^\ell)^2}{4\sqrt{2} m_{W^{(n)}}^2}, \tag{33}$$

where g is the gauge coupling constant. Note that $\delta G_F \sim (I_n^\ell)^2$ because the Fermi constant is derived from the muon lifetime. We consider only the second KK contributions for simplicity. Now the Fermi constant is related to the Peskin-Takeuchi parameters as [58]

TABLE II. Best-fit values.

$R(D)$	$R(D^*)$	$P_\tau(D)$	$P_\tau(D^*)$	$F_L(D^*)$	$\mathrm{Br}(B_c \to \tau\nu)$	χ^2_{min}/d.o.f.
0.343	0.296	0.320	−0.490	0.460	2.75×10^{-2}	1.25

$$S_{\mathrm{NMUED}} = 0, \qquad T_{\mathrm{NMUED}} = -\frac{1}{\alpha}\frac{\delta G_F}{G_F},$$
$$U_{\mathrm{NMUED}} = \frac{4\sin^2\theta_W}{\alpha}\frac{\delta G_F}{G_F}, \tag{34}$$

where we neglect possible loop effects which are subdominant compared to the tree-level contributions to δG_F. We use the data [62]

$$S = 0.05 \pm 0.11, \quad T = 0.09 \pm 0.13, \quad U = 0.01 \pm 0.11, \tag{35}$$

where the correlation coefficients are

$$\rho_{ST} = 0.90, \qquad \rho_{TU} = -0.83, \qquad \rho_{US} = -0.59. \tag{36}$$

Following the methods of Ref. [61], we impose the S, T, U constraints by requiring $\chi^2_{STU} < 6.18$ at 2σ, where χ^2_{STU} is defined by the covariant matrix relevant for the S, T, U parameters, as in Eq. (31).

The other major constraint comes from the LHC dilepton resonance searches. At the LHC the second KK gauge boson $A^{(2)}$ can be produced via the KK number violating interactions, subsequently decaying into the SM particles. Recent results from ATLAS dilepton resonance searches at 13 TeV with 13.3 fb^{-1} provide a stringent constraint on the NMUED parameters [63]. We reflect the results of Ref. [63] on the strength of the BLT in the gauge sector to constrain our analysis to the region $0 \le r_V/R \le 0.5$. The best-fit values for the minimum χ^2 are listed in Table II.

In Fig. 1 we plot the allowed regions of the NMUED parameters at the 2σ level. We scanned over the range $0 \le 1/R \le 3$ TeV. A noticeable feature is that the allowed range of r_q/R is rather narrow with negative values, contrary to that of r_ℓ/R, as shown in Fig. 1(a). In the NMUED models, $r_{q,\ell}$ are considered as free parameters and can be negative, but with some restrictions. The fields $F^{f(n)}_{L,R}$ and $G^{f(n)}_{L,R}$ of Eq. (12) have normalization factor [48–50]

$$N^f_n = \sqrt{\frac{2}{\pi R}}\frac{1}{\sqrt{1 + r_f^2 m^2_{f^{(n)}}/4 + r_f/(\pi R)}}. \tag{37}$$

For N^f_n to be meaningful, $r_f/(\pi R) > -1 - r_f^2 m^2_{f^{(n)}}/4$ and, for small values of $r_f m_{f^{(n)}}$, $r_f/R \gtrsim -\pi$. Our results in Fig. 1 satisfy this requirement. Note that the points near $r_q/R = -\pi$ are favorable for larger $R(D)$ and smaller χ^2.

Figure 2 shows the second KK masses $m_{W^{(2)}}$ and $m_{\tau^{(2)}}$. Allowed values of various observables at 2σ are given in

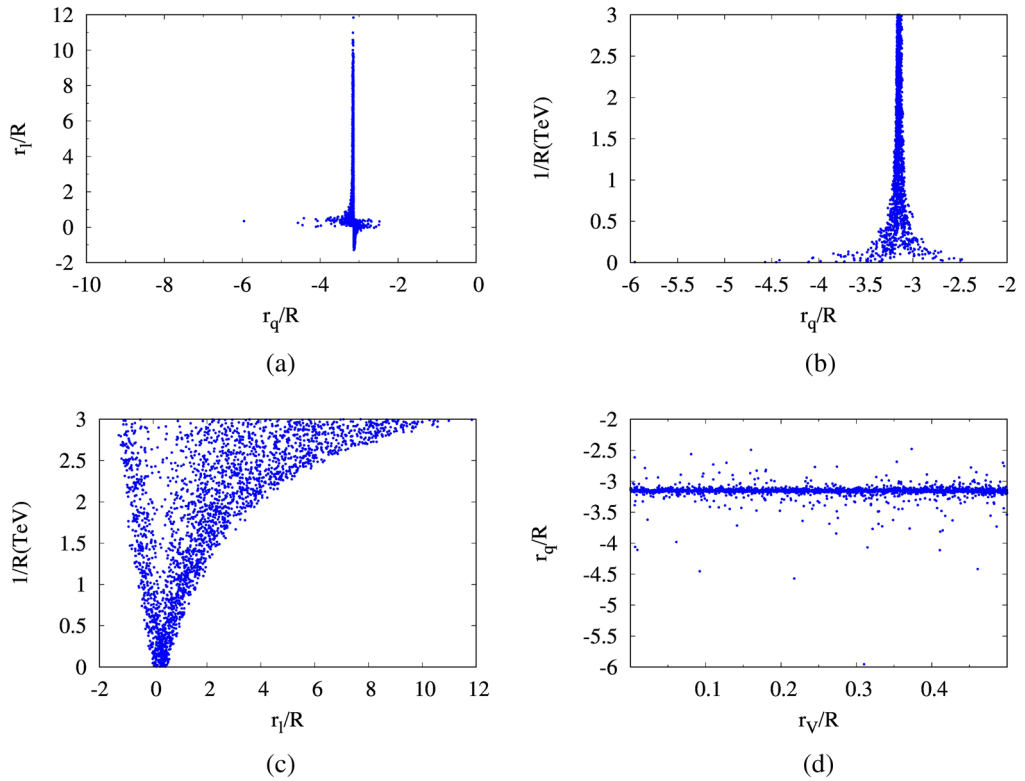

FIG. 1. Allowed regions of model parameters of NMUED at the 2σ level. (a) r_ℓ/R vs r_q/R; (b) $1/R$ (TeV) vs r_q/R; (c) $1/R$ (TeV) vs r_ℓ/R; (d) r_q/R vs r_V/R.

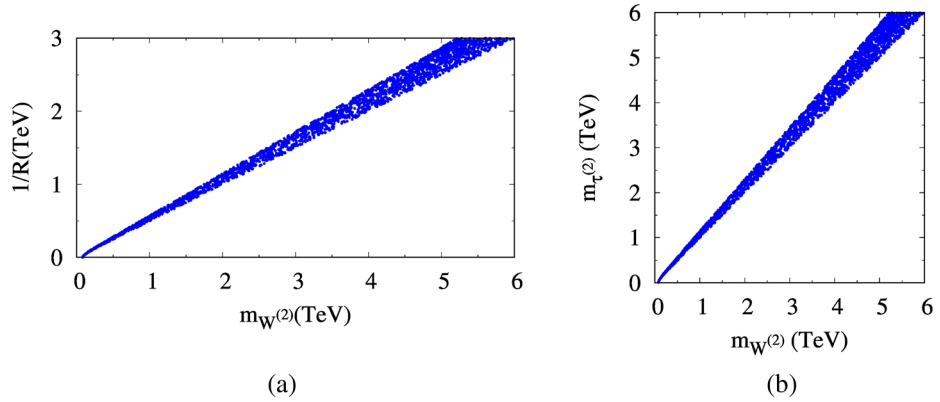

FIG. 2. Mass scales of NMUED at 2σ. (a) $1/R$ (TeV) vs $m_{W^{(2)}}$ (TeV); (b) $m_{\tau^{(2)}}$ (TeV) vs $m_{W^{(2)}}$ (TeV).

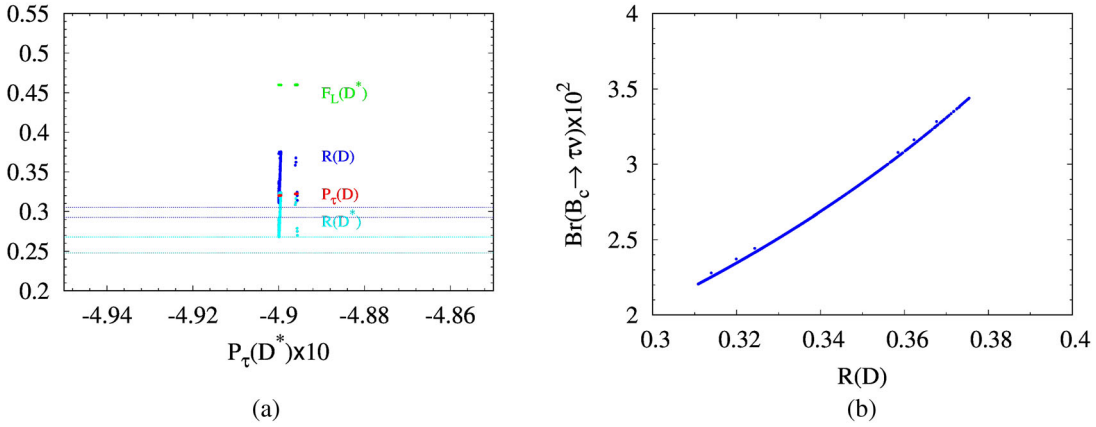

FIG. 3. Allowed values for various observables at 2σ. In (a) numerical values of $R(D^{(*)})$, $P_\tau(D)$, and $F_L(D^*)$ are plotted with respect to the values of $P_\tau(D^*)$. The horizontal lines are the SM predictions at 2σ for $R(D)$ (blue) and $R(D^*)$ (cyan). Other polarization parameters $P_\tau(D^{(*)})$ and $F_L(D^*)$ are consistent with the SM values at 2σ. In (b) the branching ratio of $\mathrm{Br}(B_c \to \tau\nu)$ vs $R(D)$ is plotted.

Fig. 3. As can be seen in Fig. 3(a), $R(D)$ is still far away from the SM predictions beyond 2σ level, while $R(D^*)$ values have small overlaps at the edge of the SM-allowed range within 2σ. But the best-fit values of $R(D^{(*)})$ in Table I are still beyond the SM by more than 2σ. Other polarization observables $P_\tau(D^{(*)})$ and $F_L(D^*)$ are consistent with the SM. Figure 3(b) shows that the branching ratio $\mathrm{Br}(B_c \to \tau\nu)$ lies safely within a few percent.

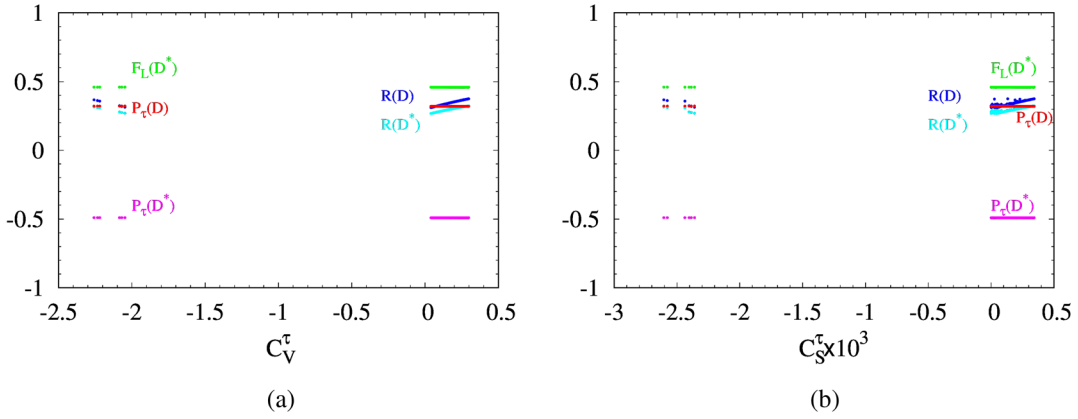

FIG. 4. Wilson coefficients $C^\tau_{V,S}$ and observables. (a) Observables with respect to C^τ_V; (b) observables with respect to $C^\tau_S \times 10^3$.

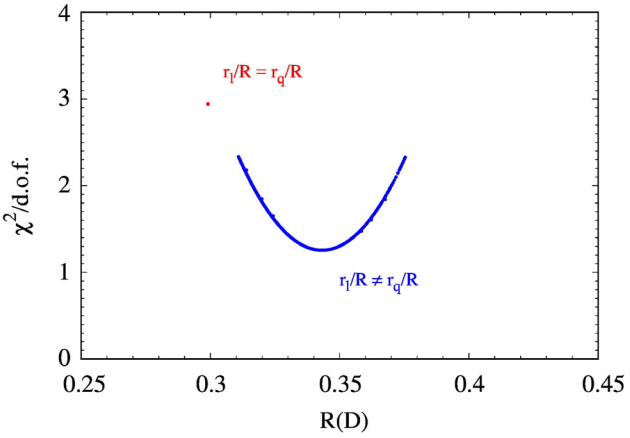

FIG. 5. $R(D)$ vs χ^2/d.o.f. for $r_\ell/R = r_q/R$ and $r_\ell/R \neq r_q/R$.

Contributions of the Wilson coefficients to observables at 2σ are depicted in Fig. 4. We find that the pattern for C_V^μ is very similar to that of C_S^μ. Note that the Wilson coefficients are

$$C_{V,S} \sim I_n^q I_n^\ell, \tag{38}$$

while the EW precision parameters are

$$T_{\mathrm{NMUED}}(U_{\mathrm{NMUED}}) \sim \delta G_F \sim (I_n^\ell)^2. \tag{39}$$

In the case of $r_q = r_\ell$ the overlap integrals become $I_n^q = I_n^\ell$ and $C_{V,S} \sim (I_n^\ell)^2$, which are directly affected by the oblique parameters of Eq. (39). According to Eq. (35), EWPT prefers small $(I_n^\ell)^2$. This means that for $r_q = r_\ell$ EWPT requires smaller $C_{V,S}$, which results in smaller $R(D^{(*)})$ and does not fit the data so well. In other words, we find that $R(D^{(*)})$ anomalies require $r_q \neq r_\ell$ in NMUED. The situation is depicted in Fig. 5, where $R(D)$ vs χ^2/d.o.f. are compared for the $r_\ell/R = r_q/R$ and $r_\ell/R \neq r_q/R$ cases.

To see the effects of $r_\ell/R \neq r_q/R$ more dramatically, we compare the cases of $r_\ell/R = r_q/R$ and $r_\ell/R \neq r_q/R$ in Fig. 6. Figure 6(a) shows that the allowed regions of r_q/R are quite different from each other. The effect of $r_\ell/R \neq r_q/R$ appears dramatically on I_2^q, as shown in Figs. 6(b)–6(d). As mentioned above, this is due to the constraints on the oblique parameters. If $r_q/R = r_\ell/R$, then $I_2^q = I_2^\ell$, and it should be kept small to satisfy the EWPT [Fig. 6(b)]. In the case of $r_q/R \neq r_\ell/R$, I_2^q can be very large compared to I_2^ℓ [Fig. 6(c)]. As a result, $R(D)$ is allowed to have large values to fit the data [Fig. 6(d)].

In our analysis $C_V^\tau = C_V^\mu$, and we checked the influence of nonzero $C_{V,S}^\mu$. Figure 7 shows some of the results. Figure 7(a) depicts $1/R$ vs r_q/R, while (b) shows $R(D)$ vs C_V^τ. We have a figure for $R(D^*)$ similar to Fig. 7(b). Whether or not $C_{V,S}^\mu = 0$ does not affect the observables

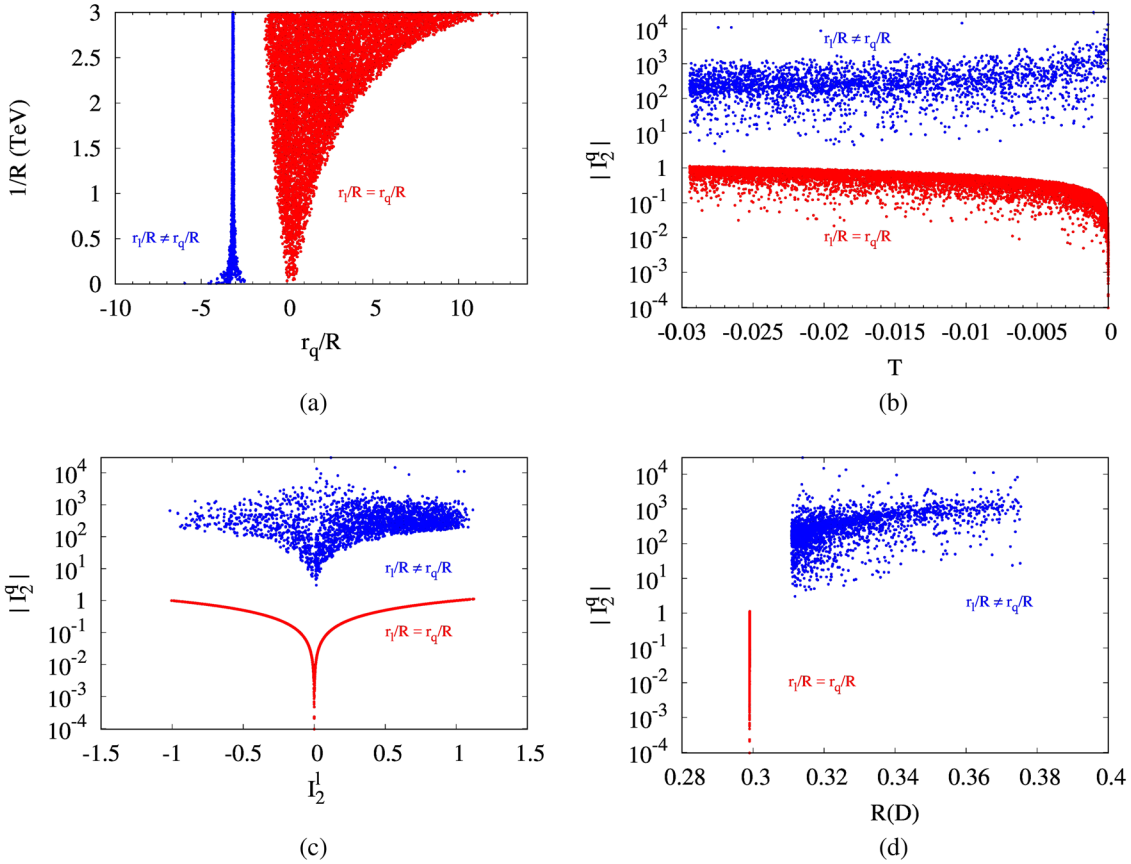

FIG. 6. Comparisons of various parameter spaces for $r_q/R = r_\ell/R$ (red) and $r_q/R \neq r_\ell/R$ (blue) at 2σ. (a) $1/R$ (TeV) vs r_q/R; (b) $|I_2^q|$ vs T; (c) $|I_2^q|$ vs I_2^ℓ; (d) $|I_2^q|$ vs $R(D)$.

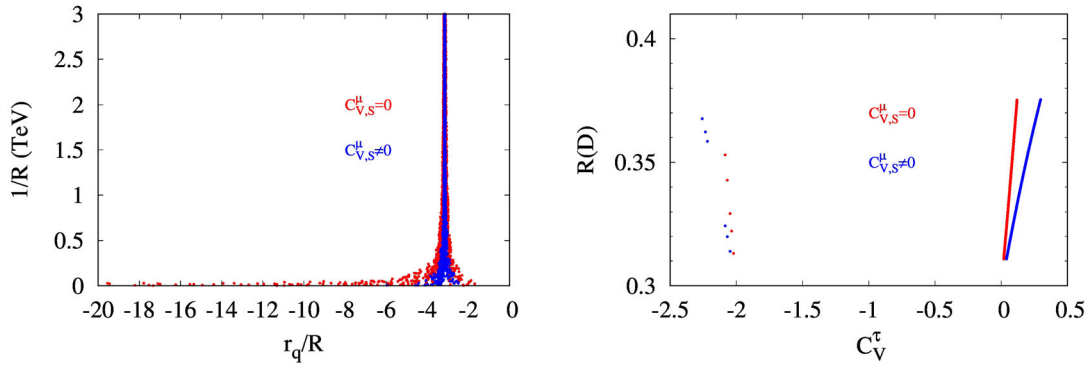

FIG. 7. Comparisons of parameter spaces for $C^{\mu}_{V,S}=0$ (red) and $C^{\mu}_{V,S}\neq 0$ (blue) at 2σ. (a) $1/R$ (TeV) vs r_q/R; (b) $R(D)$ vs C^{τ}_V.

including the polarizations so much, but the allowed range of r_q/R or C^{τ}_V could be slightly different. The effect of C^{μ}_S is negligible because its values are very small compared to C^{τ}_S. Note that C^{μ}_S is suppressed by $\sim m_{\mu}/m_{\tau}$ with respect to C^{τ}_S. And the mixed terms of $(1+C^{\mu,\tau}_V)C^{\mu,\tau}_S$ in Eq. (25) are the main source of a difference betweenthe $\tau\nu$ mode and the $\mu\nu$ mode.

In this analysis we do not consider explicitly possible constraints from the flavor changing neutral currents (FCNC) involving a b quark sector, but it needs some commentary. First, there is no FCNC at tree level because the BLT parameter r_q is flavor independent. The effective couplings of the even KK mode of gauge bosons and the SM quarks can be written as the matrix in the flavor space [51]

$$G^{(n)}=\mathrm{diag}(g^{X^{(n)}}_{r_1},g^{X^{(n)}}_{r_2},g^{X^{(n)}}_{r_3}), \tag{40}$$

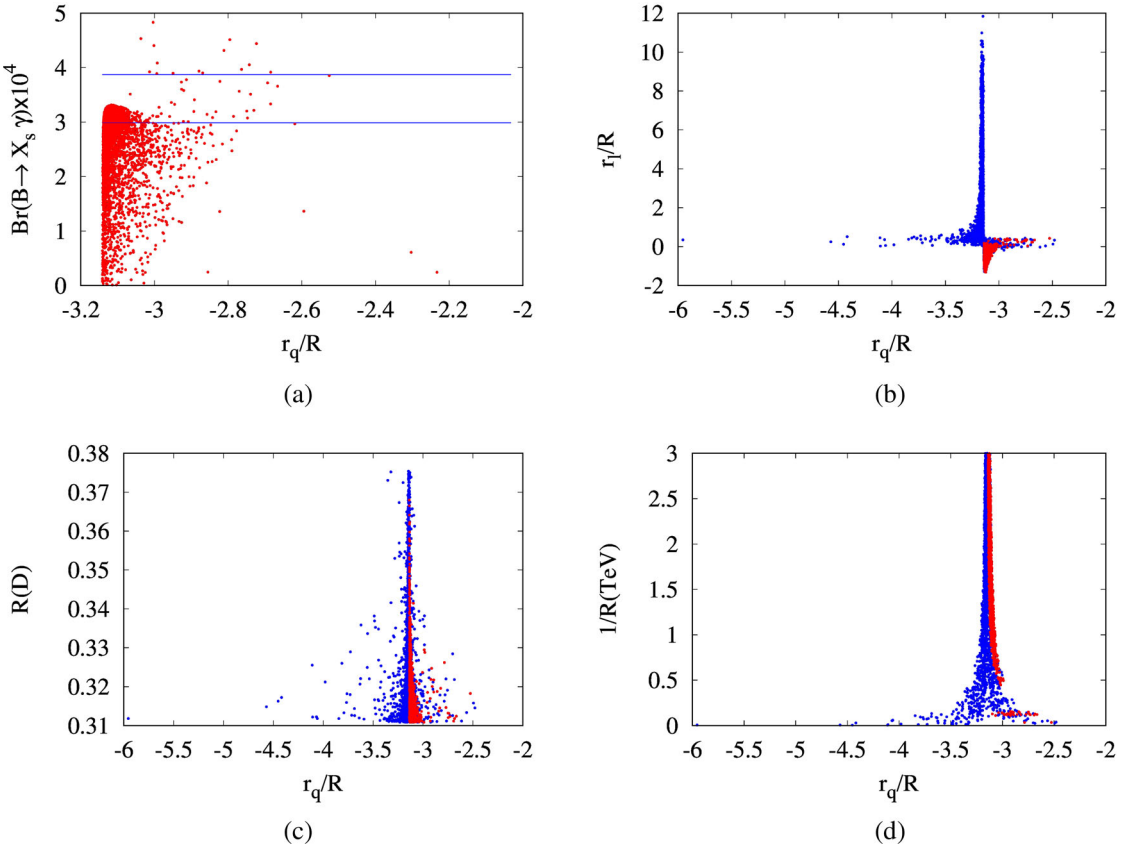

FIG. 8. Constraints from experimental results of $\mathrm{Br}(B\to X_s\gamma)=(3.43\pm 0.21\pm 0.07)\times 10^{-4}$ [49,66]. (a) Values of $\mathrm{Br}(B\to X_s\gamma)$ with the points in Fig. 1 but with $-\pi<r_q/R$. Blue horizontal lines are 2σ allowed bounds. (b)–(d) Regions allowed by $\mathrm{Br}(B\to X_s\gamma)$ (red) compared with those of Fig. 1 (blue).

where $X^{(n)} = \gamma^{(n)}, Z^{(n)}$ and $r_1 = r_2 = r_3 = r_q$ in our case. The result is that $G^{(n)}$ is proportional to the identity matrix. Second, $B_s \to \mu^+\mu^-$ and $B \to X_s\gamma$ are investigated in Refs. [48,49], respectively. The decay of $B_s \to \mu^+\mu^-$ or $B_s \to X_s\ell^+\ell^-$ involves both I_n^q and I_n^ℓ, while $B \to X_s\gamma$ involves I_n^q only. In the former case since I_n^q and I_n^ℓ both contribute to the process, one can expect that the constraint on I_n^ℓ would not be as strong as that from the oblique parameters. Actually, in Ref. [48] the analysis was done with $r_q = r_\ell$. As one can see in Fig. 6 of Ref. [48], the allowed parameter space for small r_V is compatible with our results. One point that must be noticed is that the lower limit of R^{-1} is about a few hundred GeV, which varies with r_V and $r_{q,\ell}$ (see Table II of Ref. [48]). In the case of $r_q \neq r_\ell$ the allowed parameter space would be larger. In $B \to X_s\gamma$ only I_n^q contributes to the process. According to Ref. [49], dominant contribution comes not from I_n^q but from other overlap integrals, $I_{1,2}^n$ [see Eqs. (A10) and (A11) of Ref. [49]]. The integrals contain a factor of $\sqrt{1 + r_q/(\pi R)}$, and we restrict the range of r_q as $-\pi < r_q/R$ in considering $\mathrm{Br}(B \to X_s\gamma)$. In Fig. 8 we show the effects of $\mathrm{Br}(B \to X_s\gamma)$ on parameter space. We consider only the lowest KK mode contributions for convenience. As shown in Fig. 8(b), positively large values of r_ℓ/R are not allowed. We find that a considerable amount of parameter space is forbidden, but still the value of χ^2_{min} is almost the same, and the best-fit values of the observables also remain unchanged. Third, $B_s - \bar{B}_s$ mixing involves only I_n^q and could provide a very strong constraint on r_q. The SM prediction of the mass difference ΔM_s [64],

$$\Delta M_s^{\mathrm{SM}} = (20.01 \pm 1.25)/\mathrm{ps}, \tag{41}$$

is larger by 1.8σ than the measured value [1],

$$\Delta M_s^{\mathrm{exp}} = (17.757 \pm 0.021)/\mathrm{ps}. \tag{42}$$

Usually the NP gives a positive contribution, and ΔM_s puts much stronger bounds on NP than before because the updated SM prediction of ΔM_s gets larger [65]. In our case ΔM_s is roughly $\sim (I_n^q)^4 (m_W/M_{KK})^4$, where M_{KK} is the mass of the mediating KK particle. At 2σ level, $\Delta M_s^{\mathrm{exp}}/(\Delta M_s^{\mathrm{SM}} - 2\delta\Delta M_s^{\mathrm{SM}}) - 1 \simeq 0.014$, where $\delta\Delta M_s^{\mathrm{SM}}$ is the 1σ deviation of ΔM_s^{SM}. One can naively guess that for $M_{KK} \sim 1$ TeV only order 1 of I_n^q is allowed, which could severely constrain r_q. Further study on this issue is necessary to scrutinize the model.

V. CONCLUSIONS

In conclusion, we investigated the $B \to D^{(*)}$ anomalies in the NMUED model. In the model nth KK modes of W boson and scalar couple to a pair of zero-mode fermions to result in nonzero NP Wilson coefficients. We found that the NMUED model successfully fits the current data including D^* polarizations, at the sacrifice of $r_\ell/R = r_q/R$. The EWPT plays a significant role in the model. Our main result is that the enhancement of the overlap integral in the quark sector is very crucial to explaining the B anomalies. If there would be a quite strong constraint on the quark sector (e.g., from the neutral meson mixing or whatever), then it could restrict the validity of the NMUED model seriously. We also found that the branching ratio $\mathrm{Br}(B_c \to \tau\nu)$ stays at a few percent, well below 10%. In our analysis $R(D)$ values have no overlap with the SM predictions at 2σ level, while $R(D^*)$ touches the SM-allowed region. Future measurements of more observables would check further the validity of the NMUED model.

[1] Y. Amhis *et al.* (HFLAV Collaboration), Eur. Phys. J. C **77**, 895 (2017).
[2] J. P. Lees *et al.* (*BABAR* Collaboration), Phys. Rev. Lett. **109**, 101802 (2012).
[3] J. P. Lees *et al.* (*BABAR* Collaboration), Phys. Rev. D **88**, 072012 (2013).
[4] M. Huschle *et al.* (Belle Collaboration), Phys. Rev. D **92**, 072014 (2015).
[5] Y. Sato *et al.* (Belle Collaboration), Phys. Rev. D **94**, 072007 (2016).
[6] S. Hirose (Belle Collaboration), Nucl. Part. Phys. Proc. **287–288**, 185 (2017).
[7] S. Hirose *et al.* (Belle Collaboration), Phys. Rev. Lett. **118**, 211801 (2017).
[8] S. Hirose *et al.* (Belle Collaboration), Phys. Rev. D **97**, 012004 (2018).
[9] A. Abdesselam *et al.* (Belle Collaboration), arXiv:1904.08794.
[10] R. Aaij *et al.* (LHCb Collaboration), Phys. Rev. Lett. **115**, 111803 (2015); **115**, 159901(E) (2015).
[11] R. Aaij *et al.* (LHCb Collaboration), Phys. Rev. D **97**, 072013 (2018).
[12] Average of $R(D)$ and $R(D^*)$ for Spring 2019, Heavy Flavor Averaging Group, https://hflav-eos.web.cern.ch/hflav-eos/semi/spring19/html/RDsDsstar/RDRDs.html.
[13] J. P. Lee, Phys. Rev. D **96**, 055005 (2017).
[14] A. Crivellin, C. Greub, and A. Kokulu, Phys. Rev. D **86**, 054014 (2012); **87**, 094031 (2013); A. Crivellin, J. Heeck, and P. Stoffer, Phys. Rev. Lett. **116**, 081801 (2016).
[15] P. Biancofiore, P. Colangelo, and F. De Fazio, Phys. Rev. D **87**, 074010 (2013).
[16] J. M. Cline, Phys. Rev. D **93**, 075017 (2016).

[17] M. A. Ivanov, J. G. Körner, and C. T. Tran, Phys. Rev. D **94**, 094028 (2016); **95**, 036021 (2017).
[18] C. H. Chen and T. Nomura, Eur. Phys. J. C **77**, 631 (2017).
[19] S. Iguro and K. Tobe, Nucl. Phys. **B925**, 560 (2017).
[20] I. Doršner, S. Fajfer, N. Košnik, and I. Nišandžić, J. High Energy Phys. 11 (2013) 084.
[21] R. Alonso, B. Grinstein, and J. Martin Camalich, J. High Energy Phys. 10 (2015) 184.
[22] M. Bauer and M. Neubert, Phys. Rev. Lett. **116**, 141802 (2016).
[23] R. Barbieri, G. Isidori, A. Pattori, and F. Senia, Eur. Phys. J. C **76**, 67 (2016).
[24] L. Di Luzio, A. Greljo, and M. Nardecchia, Phys. Rev. D **96**, 115011 (2017).
[25] L. Calibbi, A. Crivellin, and T. Li, Phys. Rev. D **98**, 115002 (2018).
[26] D. Bečirević, I. Doršner, S. Fajfer, N. Košnik, D. A. Faroughy, and O. Sumensari, Phys. Rev. D **98**, 055003 (2018).
[27] R. Barbieri, C. W. Murphy, and F. Senia, Eur. Phys. J. C **77**, 8 (2017).
[28] D. Buttazzo, A. Greljo, G. Isidori, and D. Marzocca, J. High Energy Phys. 11 (2017) 044.
[29] M. Bordone, C. Cornella, J. Fuentes-Martin, and G. Isidori, Phys. Lett. B **779**, 317 (2018).
[30] S. Matsuzaki, K. Nishiwaki, and K. Yamamoto, arXiv: 1903.10823.
[31] E. Megias, M. Quiros, and L. Salas, J. High Energy Phys. 07 (2017) 102.
[32] E. Megias, M. Quiros, and L. Salas, Phys. Rev. D **96**, 075030 (2017).
[33] G. D'Ambrosio and A. M. Iyer, Eur. Phys. J. C **78**, 448 (2018).
[34] M. Blanke and A. Crivellin, Phys. Rev. Lett. **121**, 011801 (2018).
[35] X. W. Kang, T. Luo, Y. Zhang, L. Y. Dai, and C. Wang, Eur. Phys. J. C **78**, 909 (2018).
[36] Z. R. Huang, Y. Li, C. D. Lu, M. A. Paracha, and C. Wang, Phys. Rev. D **98**, 095018 (2018).
[37] D. Bardhan and D. Ghosh, Phys. Rev. D **100**, 011701 (2019).
[38] M. Tanaka and R. Watanabe, Phys. Rev. D **82**, 034027 (2010).
[39] M. Tanaka and R. Watanabe, Phys. Rev. D **87**, 034028 (2013).
[40] A. Abdesselam *et al.* (Belle Collaboration), arXiv:1903 .03102.
[41] A. K. Alok, D. Kumar, S. Kumbhakar, and S. U. Sankar, Phys. Rev. D **95**, 115038 (2017).
[42] H. C. Cheng, K. T. Matchev, and M. Schmaltz, Phys. Rev. D **66**, 036005 (2002).
[43] F. del Aguila, M. Perez-Victoria, and J. Santiago, Acta Phys. Pol. B **34**, 5511 (2003).
[44] F. del Aguila, M. Perez-Victoria, and J. Santiago, J. High Energy Phys. 02 (2003) 051.
[45] T. Flacke, A. Menon, and D. J. Phalen, Phys. Rev. D **79**, 056009 (2009).
[46] A. Datta, U. K. Dey, A. Shaw, and A. Raychaudhuri, Phys. Rev. D **87**, 076002 (2013).
[47] A. Datta and A. Shaw, Mod. Phys. Lett. A **31**, 1650181 (2016).
[48] A. Datta and A. Shaw, Phys. Rev. D **93**, 055048 (2016).
[49] A. Datta, and A. Shaw (Indian Association for the Cultivation of Science Collaboration), Phys. Rev. D **95**, 015033 (2017).
[50] A. Biswas, A. Shaw, and S. K. Patra, Phys. Rev. D **97**, 035019 (2018).
[51] S. Dasgupta, U. K. Dey, T. Jha, and T. S. Ray, Phys. Rev. D **98**, 055006 (2018).
[52] T. Jha and A. Datta, J. High Energy Phys. 03 (2015) 012.
[53] M. Blanke, A. Crivellin, S. de Boer, T. Kitahara, M. Moscati, U. Nierste, and I. Nišandžić, Phys. Rev. D **99**, 075006 (2019).
[54] S. Aoki *et al.*, Eur. Phys. J. C **77**, 112 (2017).
[55] F. U. Bernlochner, Z. Ligeti, M. Papucci, and D. J. Robinson, Phys. Rev. D **95**, 115008 (2017); **97**, 059902(E) (2018).
[56] R. Alonso, B. Grinstein, and J. Martin Camalich, Phys. Rev. Lett. **118**, 081802 (2017).
[57] A. G. Akeroyd and C. H. Chen, Phys. Rev. D **96**, 075011 (2017).
[58] T. Flacke and C. Pasold, Phys. Rev. D **85**, 126007 (2012).
[59] T. Flacke, K. Kong, and S. C. Park, J. High Energy Phys. 05 (2013) 111.
[60] A. Datta, K. Nishiwaki, and S. Niyogi, J. High Energy Phys. 01 (2014) 104.
[61] U. K. Dey and T. Jha, Phys. Rev. D **94**, 056011 (2016).
[62] M. Baak, J. Cúth, J. Haller, A. Hoecker, R. Kogler, K. Mönig, M. Schott, J. Stelzer (Gfitter Group), Eur. Phys. J. C **74**, 3046 (2014).
[63] T. Flacke, D. W. Kang, K. Kong, G. Mohlabeng, and S. C. Park, J. High Energy Phys. 04 (2017) 041.
[64] L. Di Luzio, M. Kirk, and A. Lenz, Phys. Rev. D **97**, 095035 (2018).
[65] L. Di Luzio, M. Kirk, and A. Lenz, arXiv:1811.12884.
[66] Y. Amhis *et al.* (Heavy Flavor Averaging Group), arXiv: 1412.7515.